Journal of Applied Polymer Science

Indirect effect of polyvinylpyrrolidone and cetyltrimethylammonium bromide on UV-blocking efficiency of TiO_2@PVP-CTAB@SiO_2 core-shell nanohybrid particles

Mohammad Mohammadi Aslzadeh,[1] Majid Abdouss,[1] Ahmad Mousavi Shoushtari,[2] Firouz Ghanbari[3]

[1]Department of Chemistry, Amirkabir University of Technology, Tehran, Iran

[2]Department of Textile Engineering, Amirkabir University of Technology, Tehran, Iran

[3]Coating Group, Vehicle Science and Technology Research Institute, Tehran, Iran

Correspondence to: M. Abdouss (E-mail: majidabdouss@yahoo.com)

ABSTRACT: In this study, a novel and useful approach to fabricate TiO_2@PVP-CTAB@SiO_2 (TPS) nanohybrid as an effective light stabilizer agent has been reported. Also, the indirect role of the Polyvinylpyrrolidone and cetyltrimethylammonium bromide on UV (ultraviolet) protection properties of nanohybrid particles was investigated. In addition, comparative studies were carried out to evaluate the photocatalytic and UV protection properties of TiO_2@ SiO_2(TS), commercial TiO_2 (US3490), synthesized TiO_2 nanparticles, and TPS nanoparticles. Furthermore, the UV protection property of 2-(2H-benzotriazol-2-yl)−4, 6-bis (1-methyl-1-phenylethyl) phenol, as an organic anti UV, was also compared with TPS nanoparticles. The as prepared nanohybrid was characterized by Fourier transform infrared spectroscopy, zeta potential, field emission scanning electron microscope (FESEM), transmission electron microscope (TEM), and UV-Vis spectroscopy. FESEM and TEM micrographs show monodispersity and nano-metric size of TPS. Rhodamine B degradation study clearly shows that TPS present the lowest photocatalytic property. Also, UV-Vis spectroscopy results show that the TPS nanoparticles illustrate higher UV blocking ability comparing to other presented anti UV materials. TPS with convenient and useful synthesis method, high UV blocking ability, and little effect on polymer matrix can be introduced as a novel UV-blocking agent in polyurethane matrix. © 2016 Wiley Periodicals, Inc. J. Appl. Polym. Sci. **2016**, *133*, 44148.

KEYWORDS: coatings; morphology; nanoparticles; nanowires and nanocrystals; non-polymeric materials and composites; properties and characterization

Received 17 February 2016; accepted 23 June 2016

DOI: 10.1002/app.44148

INTRODUCTION

Polymeric coatings, as organic substances, are submitted to degradation during exposure to sun light or ultraviolet (UV) radiation. Degradation by UV radiation causes to loss of mechanical properties, yellowing, loss of gloss, and discoloration of coating. Generally, ultraviolet absorbers (UVAs) such as 2-(5-chloro-2H-benzotriazole-2-yl)-6-(1,1-dimethylethyl)-4-methyl-phenol, 2-(2H-benzotriazol-2-yl)-4,6-bis(1-methyl-1-phenylethyl) phenol, hydroxyphenyl-s-triazines,[1–3] and hindered amine light stabilizers (HALSs) such as bis (1,2,2,6,6-pentamethyl-4-piperidinyl) sebacate and methyl 1,2,2,6,6-pentamethyl-4-piperidyl sebacate[4] or combination of them[5] have been added to coating matrix to improve their stability against UV radiation. UVAs can improve UV stability of coating by competing with the polymer for absorption of UV light while HALSs protect coating by trapping of created free radicals.[6]

The main two drawbacks of organic UVAs are their relative high loss rate due to continuous conversion to radicals and narrow absorption peaks in UV range while inorganic UVAs present relatively wide absorption one. Generally, inorganic nano-particles such as titania,[7–10] zinc oxide,[11–14] and cerium dioxide[15,16] were used as efficient UV absorbers. In Mahltig *et al.* study[7] the combination of organic and inorganic UV absorber lead to optimized UV protection.

UV radiation, with a higher energy than inorganic oxide's band gap, creates electron–hole pair. Recombining of electron-hole pairs cause transforming of UV radiation to heat; therefore polymer matrix can be protected. In the case of titanium dioxide, these holes and electrons migrate to the surface of the particles. Created holes and electrons in the surface of particles can react with oxygen, water, or hydroxyls groups to form free radicals. These free radicals can cause degradation of organic

Additional Supporting Information may be found in the online version of this article.

molecules, which worse degradation process of coatings. To work out the problem of degradation process of coating, titanium dioxide nanoparticles has been encapsulated in inert shell. Recently, due to outstanding properties of core-shell particles, more and more studies have been focused on creating various core-shell particles such as, poly(lactic-co-glycolic acid) (PLGA) coated silica nanorattle (PLGA@SN),[17] SiO_2@SiO_2 core shell particles,[18] and SnO_2 @SiO_2 core–shell nanospheres.[19]

Core-shell particles are also interested in UV blocking field. In Ren *et al.* study,[20] the titanium dioxide nanoparticles first were coated by multilayer of polyelectrolytes, then SiO_2 shell was coated on the surface of modified TiO_2 particles. It is claimed that, after removing of polyelectrolyte layers by UV irradiation, Rattle-type TiO_2@void@SiO_2 particles were formed. In this structure, the TiO_2 core can guarantee the UV blocking activity of this nanoparticle; meanwhile, the SiO_2 shell can protect coating matrix from photocatalytic degradation of TiO_2 nanoparticles. This procedure is very complicated and expensive. Conversely, in Zhang *et al.*[21] and Bechger *et al.*[22] studies, silica (SiO_2) was used as an encapsulation shell to hybrid or coat on TiO_2, unmodified TiO_2. In the mentioned studies, sufficient analyses to prove successful synthesis of core-shell nanoparticles were not reported. Although, the procedures used in these studies are simple and less complicated. When tested, it is found that their procedure is still not appropriated for a complete coating of titanium dioxide nanoparticles. It is important to say that, incomplete coating of titanium dioxide nanoparticles is not desired in UV blocking property of synthesized core-shell nanoparticles.

In this study, a convenient and a novel approach to completely coating of TiO_2 nanoparticles by silica inert shell has been reported. In this approach first, the surface of TiO_2 nanoparticles were modified by polyvinylpyrrolidone (PVP) and cetyltrimethylammonium bromide (CTAB) stabilizers, then modified TiO_2 nanoparticles were coated by silica inert shell. Synthesized nanohybrid particles were named TPS (TiO_2@PVP-CTAB@SiO_2). TPSs nanohybrid particles were used as a new UV stabilizer agent in the matrix of PU (polyurethane) coating by in situ polymerization. In these nanoparticles, the SiO_2 inert shell can prevent the photocatalytic property of TiO_2 nanoparticles from damaging PU coating. Meanwhile, TiO_2 core improves photo stabilization of polyurethane coating during exposure to UV radiation.

EXPERIMENTAL

Materials and Methods

Titanium isopropoxide and Tetraethyl orthosilicate (TEOS) were used as titanium dioxide nanoparticles and silica source, respectively. PVP with average molecular weight of 36,000 g/mole, and CTAB were used as stabilizer. Rhodamine B (RB) was used as UV sensitive reagent. Potassium chloride (KCl) and TINUVIN were used as salt and as organic light absorber, respectively. All mentioned chemicals were obtained from Merk chemical and used as received. Ethanol (Merck Chemical, Germany) and double-distilled deionized water were used as reaction media. Two part polyurethane, 3282600000AO, was used as coating and purchased from Rangdaneh Kala CO., Iranian chemical company. Titanium dioxides nanoparticles (US 3490) were supplied from US Research Nanomaterials.

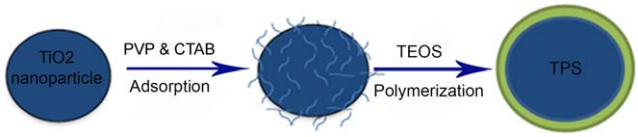

Figure 1. schematic synthesis of core – shell TPS nanocomposite particles. [Color figure can be viewed in the online issue, which is available at wileyonlinelibrary.com.]

Preparation of TiO_2 nanoparticles

TiO_2 nanoparticles were synthesized similar to method of Widoniak *et al.* study.[23] Typically, 1 mL distillated water and 0.00147 g KCl were added to 200 mL ethanol in a 250 mL reaction vessel and was mixed by magnetic stirrer for 1 h. Then, 3.4 mL Titanium isopropoxide was added dropwise in 30 min, under N_2 atmosphere. This mixture was stirred for another 12 h and the obtained sediment was washed by repeated centrifugation, decantation, and resuspension in ethanol for three times and dried overnight in vacuum oven at 40 °C. Finally, obtained powder was calcinated in a furnace at 550 °C for 5 h.

Preparation of TPS Nanocomposite Particles

A typical procedure for synthesis of TPS core-shell nanoparticles was carried out as follows: 0.01 g of TiO_2 nanoparticles (anatase form) was suspended in 16 mL of water. These nanoparticles have wide size distribution Then, PVP (0.005 g) was added to TiO_2 colloid solution and the mixture was stirred by ultrasonic and magnetic stirrer for 15 min and 24 h, respectively. Subsequently, the suspension was centrifuged and sedimented. The sediment was dispersed in the solution of 8 mL deionized water and 4 mL ethanol containing 0.048 g of CTAB. After that, 0.02 mL of ammonia was added to mentioned mixture and stirred for 1 h. Finally, 0.2 mL TEOS was added to above mixture and stirred for another 20 h. The obtained sediment was purified by repeated centrifugation, decantation, and resuspension in ethanol for three times. The products were dried in a vacuum oven overnight at 30 °C. The outline of this synthesis is shown in Figure 1. Synthesis of TS is similar to synthesis of TPS except that in synthesis of TS nanoparticles the surfaces of TiO_2 nanoparticles had been not modified by PVP and CTAB stabilizer.

Preparation of PU- TPS Nanocomposite Film

First, 0.0125 g of TPS nanoparticles was added to 1 g polyol resin solution and dispersed by ultrasonic probe for 10 min. Then 0.25 g of hardener solution, diisocyanate, was added to this mixture and mixed by high shear mixture for 10 min. Subsequently; the dispersion was coated onto a substrates with a 300 μm rod and dried at room temperature for 2 days. Other nanocomposite film samples were prepared by similar procedure.

CHARACTERIZATIONS

Fourier Transform Infrared Spectra

Fourier transform infrared (FTIR) spectra of samples were obtained on ALPHA FTIR spectrometer (Bruker Corporation) using the pressed-KBr-pellet method. Each sample was scanned 21 times with a resolution setting of 4 cm^{-1}. Spectrums were determined in the range of 400–4000 cm^{-1}.

Morphology and Elemental Analysis

transmission electron microscope (TEM) (EM10C-100 kV, Zeiss Corp., Germany) and field emission scanning electron microscope (FESEM) (Mira 3-XMU) micrographs were used to study the morphology and size of nanoparticle samples. For preparing TEM micrograph, the samples first were dispersed in ethanol media, then deposited onto carbon-coated copper grids, and dried in air. For obtaining FESEM images, nanoparticle samples were dispersed in ethanol solution by ultrasonic probe then several drops of each samples was dried on an aluminium foil. Afterward, a part of each foil samples was cut and put on a sample holder. Finally, the sample holder was coated with gold prior to examination. Energy dispersive spectroscopy (EDS) was used for elemental analysis of nanoparticle samples.

Thermogravimetric Analysis

Thermogravimetric analyses (TGA) were carried out using a thermal analysis system (STA 1500; Rheometric Scientific). The sample was dried at 100 °C for 30 min under nitrogen atmosphere before starting the experiment. TGA was carried out with 10 mg of TPS nanoparticles on a platinum pan under oxygen atmosphere with a nominal gas flow rate of 5 mL per s and heating rate of 10 °C/min.

Photocatalytic Activity

The photocatalytic property of TPS nanocomposite particles was investigated by the photo degradation of RB under UV light as follows: RB aqueous solution (10 mg/L) was added by the as obtained particles to keep the concentration of TiO_2 at 1 g/L level. The obtained mixture was stirred vigorously for 0.5 h in darkness to achieve adsorption-desorption of RB molecules on the surface of catalyst before illumination. When this dispersion was exposed to the UV irradiation, the dye molecules were decomposed. Thus, the change of dye concentration under UV irradiation could be used to evaluate and compare the photocatalytic activity of the prepared and purchased nanoparticles. The dye concentration as a function of time was measured by the UV-Vis spectrophotometer (Perkin Elmer Lambda 45, Canada) at the natural pH of the dye, room temperature and maximum absorbance of dye solution at 553 nm.

UV Shielding Performance

To study UV shielding performance of synthesized and purchased nanoparticle samples, 500 μL RB aqueous solution (5000 ppm) was mixed with 1 g part A of polyurethane using high shear mixer. Then, 0.25 g of part B of polyurethane was added to above mixture. Then, obtained mixture was sonicated for 2 min. The prepared colloidal dispersion was coated onto a glass slide with a 300 μm rod and dried at room temperature for 2 days. Finally, another mixture containing 1 g part A of polyurethane and 0.25 g of part B of polyurethane with and without nanoparticles (1 wt % of coating) was prepared and then coated onto the above dried film with the same rod to obtain nanoparticles-doped PU films and pure PU film, respectively. These films were dried at room temperature before irradiation by a UV lamp (365 nm, 20 mW/cm^2). The color changes of the samples were monitored by UV-Vis spectrophotometer at the wavelength of 553 nm.

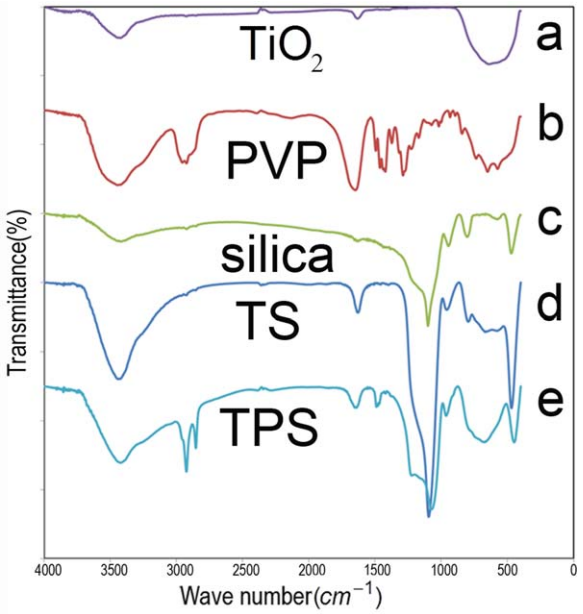

Figure 2. FTIR spectra of (a) TiO_2 (b) PVP (c) silica (d) TS (e) TPS. [Color figure can be viewed in the online issue, which is available at wileyonlinelibrary.com.]

The Zeta Potential

The measurement of the ζ-potential of the aqueous suspensions of TPS was carried out on a Malvern Zetasizer Nano-ZS (Malvern Instruments, Malvern, Worcestershire, UK). The zeta potential of the TPS nanoparticles was measured at natural Ph of TPS and temperature of 25 °C.

RESULTS AND DISCUSSION

FTIR Analysis

The chemical nature of the samples was verified by FTIR spectra. Figure 2 shows the FTIR spectra of TiO_2, SiO_2, PVP, TS, and TPS in the region of 400–4000 cm^{-1}. Figure 2(a) shows FTIR spectrum of TiO_2 nanoparticles. The broad band between 400 and 880 cm^{-1} is due to Ti—O—Ti stretch vibration.[24] This broad band also appeared in FTIR spectra of the nanocomposite particles around 400–900 cm^{-1}. This peak clearly shows that the composition of TiO_2 nanoparticles did not change after coating with silica shell. The absorption peaks at 3487 and 1658 cm^{-1} are due to stretching and bending vibration of —OH groups, respectively. These peaks could be related to —OH groups on the surface of nanoparticles and residual water. Figure 2(b) shows FTIR spectrum of PVP, the appeared broad band at 3516 cm^{-1} is related to the stretching vibration of the O—H bond of the adsorbed water molecules. Asymmetric stretching of CH_2 and C—H stretching vibration are observed at around of 2977 cm^{-1}. The vibration band at 1690 cm^{-1} is attributed to either C—N or C═O functional groups. CH_2 wagging and scissoring are appeared at 1267 and 1452 cm^{-1}, respectively. As shown in Figure 2(c), the asymmetric and symmetric stretching vibration of Si—O—Si bond and symmetric stretching of the Si—OH bond appeared in about 1111, 828, and 1011 cm^{-1},[25] respectively. Mentioned peak indicate that SiO_2 nanoparticles were successfully synthesized. Figure 2(d)

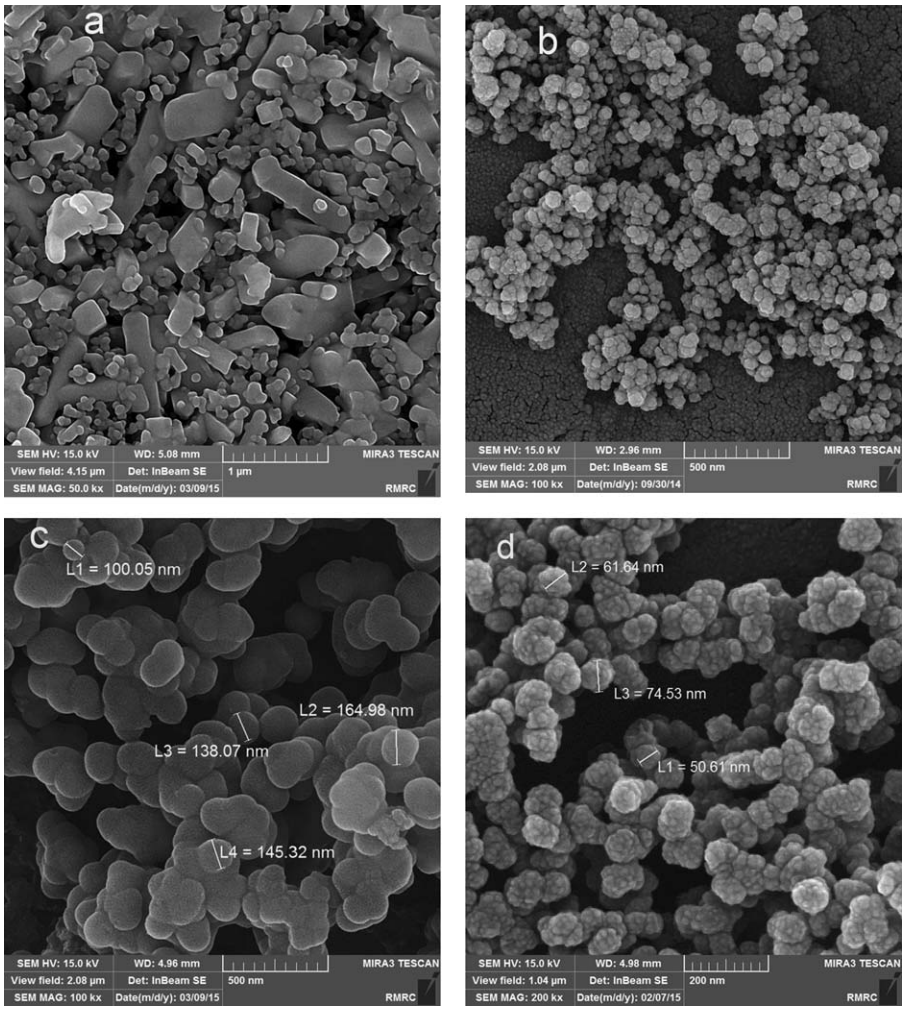

Figure 3. FESEM images of (a) TiO_2 (polydisperse) (b) TiO_2 (30 ± 5 nm) (c) TPS (d) TS.

indicates the spectrum of TS nanocomposite. As can be seen, all peaks related to TiO_2 and SiO_2 were appeared in this spectrum. The appeared peak in 1103, 819, and 1011cm^{-1} as well as the broad band between 400 and 907 cm^{-1} are due to asymmetric and symmetric stretching vibration of Si—O—Si bond, symmetric stretching of the Si—OH bond, and Ti—O—Ti stretch vibration mode, respectively. It can be concluded that TS nanoparticles was successfully synthesized. Figure 2(e) shows FTIR spectrum of TPS. As shown in this figure the asymmetric and symmetric stretching vibration of Si—O—Si bond were appeared in about 1103 and 815 cm^{-1}, respectively. The absorption peak in 1007 assigned to symmetric stretching of the Si—OH bond. The sharp adsorption peak in 477 cm^{-1} is related to the O—Si—O bending vibration. The absorption peaks in 2914–2934 cm^{-1} are due to sp3 C—H stretching vibration of PVP and CTAB, and a strong broad absorption peaks at centred around 3481cm^{-1} and 1654 cm^{-1} are due to stretching and bending vibration of —OH groups, respectively. Mentioned peaks imply successful synthesis of TPS nanoparticle. This finding is promising of formation of TPS and TS core-shell nanoparticles.

FESEM Micrographs

FESEM images of TiO_2 (polydisperse), TiO_2 (30 ± 5 nm), TPS, and TS are shown in Figure 3(a–d) respectively. Figure 3(a,b) show polydisperse and monodisperse TiO_2 nanoparticle samples, respectively. The small particles on top of the nanoparticles in Figure 3(b,d) may be related to the gold layer which was applied in coating of sample for conducting of nanoparticle samples. TiO_2 nanoparticles, shown in Figure 3(b), were used for preparation of core-shell nanoparticle samples. The measurements of image analyzer software (Image J) show that the average particles size of TS and TPS is about 100 and 220 nm, respectively. Obtained nanocomposite particles were larger than original TiO_2 nanoparticles, which were about 30 nm. Increasing of particles size clearly shows that silica shell was successfully coated on the surface of TiO_2 nanoparticles. The measurements of image analyzer software (Image J) show that shell about 35 and 80 nm was formed. In Wang *et al.* study,[26] some of Cu^{2+} ions was transformed to CuS (Copper sulphide), which act as nucleus for further grows. In Koley *et al.* work,[27] similarly many small particles of FY (phenylalanyl-tyrosine) dipeptide act as nucleus for the formation of large flat plates.

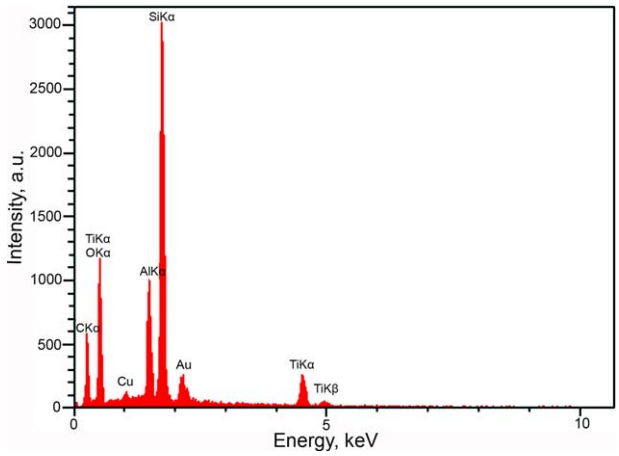

Figure 4. Quantitative analysis of core shell nanoparticles. [Color figure can be viewed in the online issue, which is available at wileyonlinelibrary.com.]

As shown in Figure 3(c,d), the nanoparticles with size of titanium dioxide nanoparticles do not exist. According to mentioned studies,[26,27] absence of nanoparticles with size of original titanium dioxide may imply this phenomenon that titanium dioxide nanoparticles act as nucleus for further grows by polymerization of TEOS and formation of silica shell. It can be seen that TS and TPS nanoparticles remained at a relatively narrow size distribution. Quantitative analysis of the C, O, Al, Si, and Ti in core-shell nanoparticles are shown in Figure 4. The Al comes from the aluminium foil, O related to SiO_2 and TiO_2, C comes from unreacted alkyl chain in TEOS and Titanium isopropoxide, CTAB, PVP, and carbon film on the FESEM holder, Ti and Si comes from titanium dioxide core and silica inert shell, respectively. The presence of Au and Cu is due to Au coating layer and FESEM cupric holder, respectively. Quantitative data show that core-shell nanoparticles composition of TPS is Ti:Si 1:3.74 ratio. Calculated Si per g of Ti is obtained by eq. (1), derived in this work:

$$\text{Calculated Si per 1 g of Ti} = \frac{n\,\text{mL TEOS}}{m\,\text{g TiO}_2} \times 0.2108 \qquad (1)$$

where n, m, and 0.2108 are the millilitres of TEOS, the grams ofTiO_2, and constant number calculated with regard to molar mass and atomic weight of molecules and atoms, respectively. Calculated composition of TPS was estimated with regard to recipe mentioned in experimental section and assumption which the TEOS polymerization reaction cloud reach 100% efficiency is Ti:Si 1:4.22 ratio. The difference between quantitative data from EDS and calculated one may be related to lower TEOS polymerization reaction efficiency and losing of some very fine SiO_2 nanoparticles during washing by repeated centrifugation, decantation, and resuspension.

TEM Micrographs

TEM micrographs were provided to prove the obtained results of FTIR and FESEM and further investigation. Figure 5(a,b) show TEM micrographs of TS nanocomposite particles in two magnifications. As shown in Figure 5(b), some of TiO_2 nanoparticles were not completely covered by silica inert shell and uncoated part of surface of these TiO_2 nanoparticles appeared dark in TEM micrograph, due to higher atomic number of Ti than Si (marked by black arrow in Figure 5(b), conversely, some part of surface of TiO_2 nanoparticles core was coated by silica. Silicon has lower atomic number in comparison with titanium and as a result, silica shell appeared gray (marked by yellow arrow in Figure 5(b). These figures clearly indicate that the direct polymerization of TEOS on the surface of unmodified TiO_2 nanoparticles is not a proper procedure for preparation of core-shell nanoparticles because some parts of titanium dioxide nanoparticles can not entirely be coated with silica shell. This is beside high capability for new silica particles formation, which cannot be distinguished from core shell nanoparticles by FESEM micrograph. The TEM micrograph of TS shows that the surface of unmodified TiO_2 nanoparticles is not suitable enough to be entirely coated by silica inert layer. In this case, one of interesting strategy is modification of nanoparticles surface by an effective stabilizer. In Graf *et al.* study,[28] the surface of various colloidal particles such as small gold colloids, small and large silver colloids, gold-shell silica-core particles, gibbsite platelets, boehmite rods, and positively or negatively charged polystyrene were modified by PVP to prepare related core-shell particles.

Considering their results, TiO_2 nanoparticles surface were first modified by PVP and CTAB stabilizer and then were coated by silica inert shell.

As shown in Figure 5(c,d), TEM images show a core–shell structure with TiO_2-core (dark) and Si-shell (gray). As can be seen, titanium dioxide nanoparticles were completely coated by silica inert layer. It also can be seen that any core-shell nanoparticle contains one or several cores. The measurements of image analyzer software (Image J) show that shell thickness of nanoparticles is about 60 nm. These micrographs demonstrate that surface modification of titanium dioxide nanoparticles prevented the formation of new silica nanoparticles and silica source was completely consumed only in formation process of core-shell nanoparticles. Compared with the TS nanoparticles, presence of PVP and CTAB in TPS preparation recipe, obviously increase the mean particles size of TPS. This result may be related to presence of several titanium dioxide nanoparticles as core in TPS nanoparticles. Figures 5(b,e) show that TiO_2 cores of the TPS and TS have wide size distribution. The measurements of image analyzer software (Image J) show that the sizes of utilized TiO_2 nanoparticles in TPS and TS are in the range of 15–60 nm. Obtained results in this study show that FTIR spectroscopy is not sufficient to prove the successful formation of core-shell nanoparticles.

The Zeta Potential

Zeta potential is a useful indicator of surface charge of particles and nanoparticles. Moreover, it can be used to predict the stability of colloidal suspensions or emulsions. In other word, zeta potential is the key factor to predict dispersion or aggregation of particles in liquid media. Essentially greater zeta potential leads to higher stability of particles in liquid media. The charged particles repel one another and thus overcome the natural tendency to aggregate. The zeta potential of TPS nanoparticles was equal to 15.2. Obviously, the obtained result meets

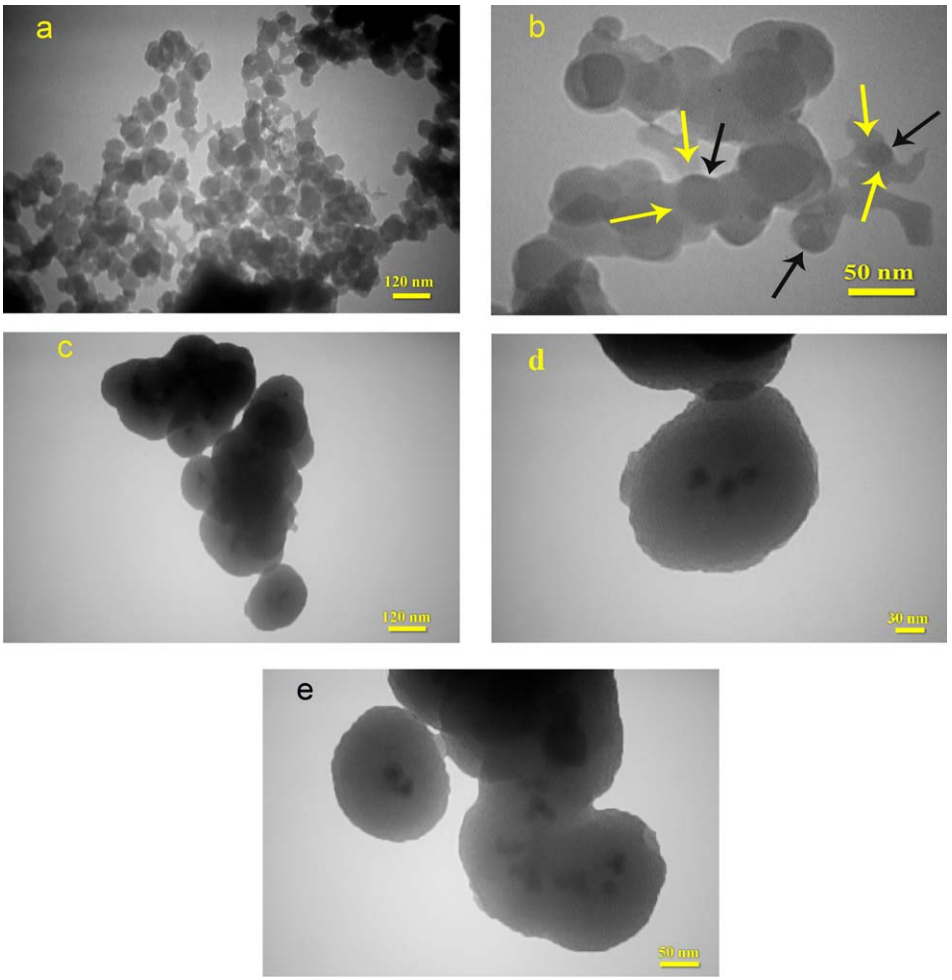

Figure 5. TEM micrographs of (a) TS composite particles (b) dotted line area marked in (a) in higher digital magnification(c) and (d) TPS nanocomposite particles in two magnification (e) TPS with various size of TiO_2. [Color figure can be viewed in the online issue, which is available at wileyonlinelibrary.com.]

the quality and indicated the small amount of aggregation. The mentioned zeta potential is almost in the range of "delicate dispersion" rather than flocculation.[29] The obtained zeta potential shows that some of TPS nanoparticles maybe are being agglomerated in the photocatalytic activity test. Therefore, TPS colloid solution was sonicated before photocatalytic activity test, to prevent agglomeration of TPS colloid solutions.

TGA Analysis

The thermogravimetric curve of TPS nanoparticles are shown in Figure 6. This curve was obtained at a heating rate of 10 °C/min under oxygen atmosphere. The TGA curve of TPS exhibits at least three steps degradation process. The TGA curve of TPS indicates a mass loss of about 2.1 wt % before 200 °C, can be attributed to the loss of water and solvent from the sample. The second loss of about 22 wt % occurred between 200–440 °C, which is due to complete degradation of CTAB[30] and first step degradation of PVP. For CTAB, the complete decomposition take place in the range of 200–400 °C and the maximum of peak is at 279 °C.[30] In oxygen atmosphere, the PVP exhibits a complex curve with at least two distinct steps[31]: In the first step, the PVP begins to lose weight at 250 °C and continues up to 440 °C with a total weight loss about 70 wt %. The second step degradation of PVP commences from 440 and continues up to 550 °C, with loss about 30 wt %. The third loss of TPS takes place in the range of 440–550 °C, is about 4 wt %. The third loss of TPS also can be related to second step degradation of PVP. From room temperature to 800 °C, the complete weight loss for TPS is about 30 wt %. The final residual weight of TPS in 800 °C is attributed to presence of $TiO_2$and SiO_2 compounds. In Zhang *et al.*[32] study, bare silica shows about 2.4 wt % loss, attributed to the reduction of the silanol groups.[33] In Massard *et al.* study, TiO_2 nanoparticles show about 1 wt % loss.[34]

Photocatalytic Activity of the TPS Nanoparticles

It is critical that photo stabilizer nanoparticles have the lowest photocatalytic activity. Degradation of RB, as sensitive and model molecule, was evaluated to study the photocatalytic behavior of the TPS and TS core-shell nanoparticles. For further investigation and controlling the photocatalytic activity test, TiO_2 nanoparticles in two nanometric size were studied. Figure 7 indicate the normalized photocatalytic degradation profiles of RB with equal amount of TPS, TS, TiO_2, and a blank test. A and A0 represent the absorbances of the dye at any time and in the initial time of UV irradiation, respectively; thus, A/A0 indicates the ratio of the remaining concentration to the initial concentration of the dye in the solution. As can be seen, RB was

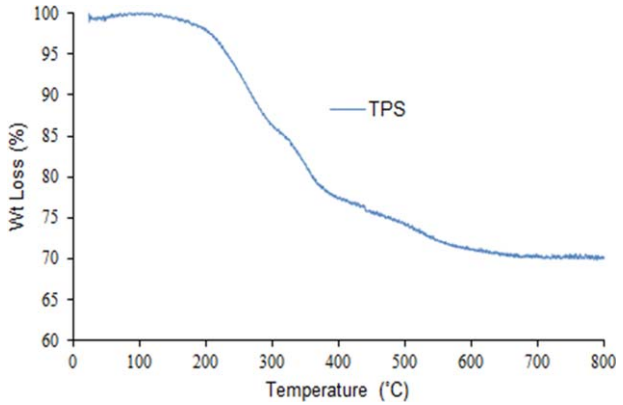

Figure 6. TGA curve of TPS. [Color figure can be viewed in the online issue, which is available at wileyonlinelibrary.com.]

hardly decomposed under UV irradiation in the absence of any catalyst. For the TiO_2— catalyzed systems, the relative degradation rate of the RB is in the order of: US 3490 > TiO_2 anatase form > TS > blank > TPS. These results show that TPS does not present any photocatalytic activity; however, illustrate UV shielding property. In TPS nanocomposite particles, the surface of titanium dioxide nanoparticles were completely wrapped by silica inert layer. Silica inert layer shields the active sites of TiO_2 nanoparticles. The second outcome of this test is related to the effect of the particle size in photocatalytic properties. As the size of titanium dioxide nanoparticles decrease, the photocatalytic activities of nanoparticles were increased. This result is related to this fact that the specific surface area of smallest nanoparticles and as a result the number of active surface sites is higher than larger one. This finding is in agreement with the finding of Liao and Liao[35] and Zhang *et al.*[36] studies. However, it is important to say that the photocatalytic activity does not monotonically increase with decreasing of particle size, and there is an optimum particle size for TiO_2 photocatalyst.[37] As shown in Figure S1 (S mean Supporting Information) more intuitionistic visualization can be compared from the corresponding color changes between

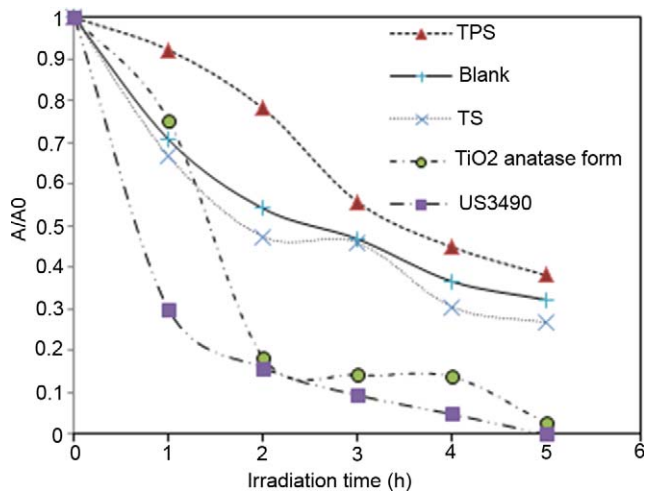

Figure 7. Normalized photocatalytic degradation profiles of RB, TPS (▲) blank (+) TS (×) TiO_2 anatase form (●) US3490 (■). [Color figure can be viewed in the online issue, which is available at wileyonlinelibrary.com.]

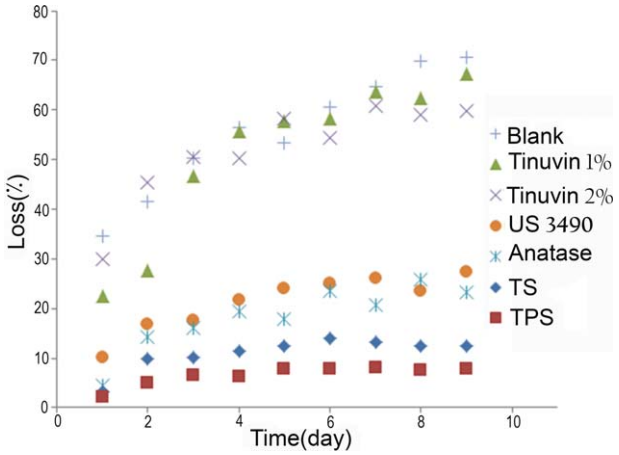

Figure 8. loss percent of RB absorbance of the Rhodamine B-doped PU film as a substrates of blank-PU (+), TIN1%-PU (▲), TIN2%-PU (×), US3490-PU (●), anatase-PU (*)TS-PU (◆)TPS-PU (■). [Color figure can be viewed in the online issue, which is available at wileyonlinelibrary.com.]

solutions of TPS, TS, TiO_2anatase form, US 3490, and blank. Obtained results imply that TPS is a promising novel UV stabilizer without photocatalytic property.

UV-Shielding Property

To determine the actual UV protection effect of TPS nanoparticles, a UV-sensitive material, RB-doped PU film, was used as the substrates of the TPS-doped PU film. To further investigation and to compare the results, pure PU film, various UV stabilizer-doped PU films, and nanoparticles- doped PU films were used as protecting layer of RB- doped PU film. The photodegradation of dye-doped films as a function of irradiation time were measured by monitoring the maximum absorption intensity at 553 nm. As shown in Figure 8, after irradiation for 9 days, the TINUVIN doped PU films and pure PU protected film show more than 50% of loss while the film protected TPS-doped PU film only show 8% of loss. The relative loss rate of the RB was in the order of: blank > TINUVIN 1% wt > TINUVIN 2% wt > US 3490>TiO_2 anatase form > TS > TPS. Nanocomposite particles show better UV-shielding performance in comparison with TINUVIN 234. The obtained results clearly show that organic UV absorbers are not as useful as nanoparticles. According to results of photocatalytic activity of the TPS nanoparticles section, US 3490 and titanium dioxide nanoparticles (anatase form) show high photocatalytic activity. Anyhow, as shown in Figure 8 these nanoparticles present better UV shielding properties than TINUVIN 234. This study shows that inorganic anti UV such as titanium dioxide can strongly protect polymeric coating from UV radiation in comparison with organic anti UV. This finding is in agreement with Forsthuber *et al.* study.[38] The main disadvantage of coating incorporated with titanium dioxide nanoparticles is the hazy appearance of those films. This appearance has been related to the reflection property of titanium dioxide nanoparticles in the visible region, where have weak absorption property.[9]

Obtained results show that UV shielding properties of TiO_2 nanoparticles can be improved by encapsulation of them in inert shell such as silica shell. This improvement is not related to higher

absorbance ability of core-shell nanohybrid in UV region. Higher UV shielding properties of TPS and TS in comparison with TiO_2 nanoparticles related to their ability to suppress photocatalytic activity of TiO_2 nanoparticles core. Moreover, by comparing the results of the actual UV protection effect of TPS with TS, one can conclude that the quality of encapsulation is a key factor in UV shielding activity of titanium dioxide nanoparticles.

CONCLUSIONS

In this work, TS and TPS core-shell nanocomposite particles were synthesized by encapsulation of TiO_2 nanoparticles into SiO_2inert shell. TEM micrographs show that PVP and CTAB illustrate very key role in complete coating of titanium dioxide nanoparticles by silica inert shell. This study also shows that inorganic light stabilizer can strongly protect polymeric coating from UV radiation in comparison with organic light stabilizer. The results of degradation of RB test shows that the TPS nanohybrid composite particles have UV-shielding property without any photocatalytic activity. The obtained data from UV-shielding property experiment present that TPS-doped PU films show the highest UV shielding property. High UV-shielding property and low photocatalytic activity of TPS makes it a very effective UV stabilizer for polymeric coatings.

ACKNOWLEDGMENTS

The authors are grateful to the Renewable Energy Research Center (RERC) (Tehran, Iran) for the financial support of this work.

REFERENCES

1. Goldshtein, J.; Margel, S. *Colloid Polym. Sci.* **2011**, *289*, 1863.
2. Aslzadeh, M. M.; Abdouss, M.; Shoushtari, A. M.; Ghanbari, F. *Iran. Polym. J.* **2016**, *25*, 145.
3. Schaller, C.; Rogez, D.; Braig, A. *J. Coat. Technol. Res.* **2007**, *5*, 25.
4. Nguyen, T. V.; Nguyen Tri, P.; Nguyen, T. D.; El Aidani, R.; Trinh, V. T.; Decker, C. *Polym. Degrad. Stab.* **2016**, *128*, 65.
5. Jia, H.; Wang, H.; Chen, W. *Radiat. Phys. Chem.* **2007**, *76*, 1179.
6. Decker, C.; Biry, S.; Zahouily, K. *Polym. Degrad. Stab.* **1995**, *49*, 111.
7. Mahltig, B.; Böttcher, H.; Rauch, K.; Dieckmann, U.; Nitsche, R.; Fritz, T. *Thin Solid Films* **2005**, *485*, 108.
8. Han, K.; Yu, M. *J. Appl. Polym. Sci.* **2006**, *100*, 1588.
9. Yang, H.; Zhu, S.; Pan, N. *J. Appl. Polym. Sci.* **2004**, *92*, 3201.
10. Xiao, X.; Liu, X.; Cao, G.; Zhang, C.; Xia, L.; Xu, W.; Xiao, S. *Polym. Eng. Sci.* **2015**, *55*, 1296.
11. Lee, S. *J. Appl. Polym. Sci.* **2009**, *114*, 3652.
12. Lizundia, E.; Ruiz-Rubio, L.; Vilas, J. L.; León, L. M. *J. Appl. Polym. Sci.* **2016**, *133*, DOI: 10.1002/app.42426.
13. Rangari, V. K.; Mohammad, G. M.; Seyhan, B.; Jeelani, S. *J. Appl. Polym. Sci.* **2013**, *129*, 121.
14. Hang, T. T. X.; Dung, N. T.; Truc, T. A.; Duong, N. T.; Van Truoc, B.; Vu, P. G.; Hoang, T.; Thanh, D. T. M.; Olivier, M. G. *Prog. Org. Coat.* **2015**, *79*, 68.
15. Li, C.; Shu, S.; Chen, R.; Chen, B.; Dong, W. *J. Appl. Polym. Sci.* **2013**, *130*, 1524.
16. Saadat-Monfared, A.; Mohseni, M.; Tabatabaei, M. H. *Colloids Surf. A* **2012**, *408*, 64.
17. Li, L.; Zhang, Y.; Hao, N.; Chen, D.; Tang, F. *Chin. Sci. Bull.* **2012**, *57*, 3631.
18. Zhang, Q.; Ge, J.; Goebl, J.; Hu, Y.; Lu, Z.; Yin, Y. *Nano Res.* **2009**, *2*, 583.
19. Wang, L.; Fei, T.; Deng, J.; Lou, Z.; Wang, R.; Zhang, T. *J. Mater. Chem.* **2012**, *22*, 18111.
20. Ren, Y.; Chen, M.; Zhang, Y.; Wu, L. *Langmuir* **2010**, *26*, 11391.
21. Zhang, Y.; Yu, L.; Ke, S.; Shen, B.; Meng, X.; Huang, H.; Lv, F.; Xin, J.; Chan, H. L. W. *J. Sol-Gel Sci. Technol.* **2011**, *58*, 326.
22. Bechger, L.; Koenderink, A. F.; Vos, W. L. *Langmuir* **2002**, *18*, 2444.
23. Widoniak, J.; Eiden-Assmann, S.; Maret, G. "Influence Of Additives on Size and Porosity in the Synthesis of Uniform TiO_2 Nanoparticles," in Mesophases, Polymers, and Particles. vol. 129, ed: Springer Berlin Heidelberg, **2004**, pp 119–125.
24. Li, X.; Wang, D.; Luo, Q.; An, J.; Wang, Y.; Cheng, G. *J. Chem. Technol. Biotechnol.* **2008**, *83*, 1558.
25. Sun, J.; Yu, G.; Liu, L.; Li, Z.; Kan, Q.; Huo, Q.; Guan, J. *Catal. Sci. Technol.* **2014**, *4*, 1246.
26. Wang, M.; Sun, L.; Fu, X.; Liao, C.; Yan, C. *Solid State Commun.* **2000**, *115*, 493.
27. Koley, P.; Sakurai, M.; Aono, M. *J. Mater. Sci.* **2015**, *50*, 3139.
28. Graf, C.; Vossen, D. L. J.; Imhof, A.; van Blaaderen, A. *Langmuir* **2003**, *19*, 6693.
29. Riddick, T. M.; Ravina, L. A. *Ind. Eng. Chem.* **1970**, *62*, 70.
30. Zhang, T.; Xu, G.; Puckette, J.; Blum, F. D. *J. Phys. Chem. C* **2012**, *116*, 11626.
31. Peniche, C.; Zaldívar, D.; Pazos, M.; Páz, S.; Bulay, A.; Román, J. S. *J. Appl. Polym. Sci.* **1993**, *50*, 485.
32. Zhang, H.; Li, C.; Guo, J.; Zang, L.; Luo, J. *J. Nanomater.* **2012**, *1*, 2012.
33. Mueller, R.; Kammler, H. K.; Wegner, K.; Pratsinis, S. E. *Langmuir* **2003**, *19*, 160.
34. Massard, C.; Bourdeaux, D.; Raspal, V.; Feschet-Chassot, E.; Sibaud, Y.; Caudron, E.; Devers, T.; Awitor, K. O. *Adv. Nanopart.* **2012**, *1*, 86.
35. Liao, D. L.; Liao, B. Q. *J. Photochem. Photobiol. A* **2007**, *187*, 363.
36. Zhang, Q.; Ge, J.; Goebl, J.; Hu, Y.; Lu, Z.; Yin, Y. *Nano Res.* **2010**, *2*, 583.
37. Zhang, Z.; Wang, C. C.; Zakaria, R.; Ying, J. Y. *J. Phys. Chem. B* **1998**, *102*, 10871.
38. Forsthuber, B.; Schaller, C.; Grüll, G. *Wood Sci. Technol.* **2013**, *47*, 281.